ENGINEERING ELECTROACTIVE BACTERIAL CELLULOSE-CARBON NANOTUBE BANDAGES FOR TREATMENT OF STAPHYLOCOCCUS AUREUS

DANIEL LEVIN

Society for Science and the Public

Abstract

Staphylococcus aureus hospitalizes over 320,000 people yearly, is becoming increasingly resistant to gold-standard antibiotics like vancomycin, and can stop wounds from healing. In this study, bacterial cellulose-carbon nanotube (BC-CNT) bandages were engineered to produce electrochemical species, which rapidly eliminated vancomycin-intermediate *S. aureus*. To create the bandages, the bacteria *K. sucrofermentans* was cultured to synthesize a BC membrane. Then, CNTs—one of the most electrically conductive materials at room temperature—were integrated into decellularized BC. This created stable and electrically conductive BC-CNT bandages. The electrical properties were then modeled and used to design circuitry throughout the bandages. When *S. aureus* was exposed to the electrified bandages for just an hour, its biofilm-forming capacity decreased by over 91% and displayed increased antibiotic susceptibility. This effect was most prominent in areas of reduced pH, implying that the electric signals generate antimicrobial compounds and disrupt transcellular charge gradients that underpin *S. aureus* homeostasis. These results advance applications of electrochemistry in medicine and create a new direction to overcome antibiotic-resistant infections.

Introduction

Antibiotic-Resistant Infection

Within the next thirty years, antimicrobial-resistant infection (AMR) will likely become deadlier than cancer.[1] AMR killed 1.27 million people in 2019, contributing to more deaths than HIV/AIDS or malaria.[2] 331,470 of these deaths were directly attributed to the bacterial pathogen *Staphylococcus aureus*.[2] *S. aureus* is found in 65% of chronically infected wounds and can stop the healing process by forming biofilms.[3,4] Bacteria in biofilms can be 10–1,000-fold more resistant to antibiotics than their planktonic counterparts.[5,6] Extracellular polymeric substances (EPS, made up of amyloidogenic proteins, exopolysaccharides, or e-DNA) allow *S. aureus* to aggregate in biofilms, activate genes that confer antibiotic resistance, and prevent epithelial cell migration and immune cell penetration which inhibit film clearance.[7,8] EPS also creates a hypoxic and nutrient-depleted environment that suppresses centralized *S. aureus* cells into metabolic dormancy.[9] This sub-population of cells—persister cells—becomes invulnerable to antibiotics and can cause recurrent infection following initial biofilm clearance.[10] There is not a sufficient number of drugs in development to keep up with the proliferation of antibiotic resistance.[11] This research addresses this problem by developing a treatment to control antibiotic-resistant bacteria without using antibiotics and by using pre-existing antibiotics in new ways.

Chemical and Electrical Bactericide

Low-level electrical currents can impair biofilm and persister cell formation.[12] Electricity can hydrolyze water and generate reactive oxygen species (ROS) such as hydrogen peroxide.[13,14] ROS can mutate DNA, and induce oxidative stress and autolysis in bacterial cells.[15,16] Micro-amperage electrical currents successfully disrupt control over ion, protein, and antibiotic transport through bacterial cell membranes, which can overpower cell membrane-dependent mechanisms of drug evasion.[17,18] Many studies use inert electrodes made of silver, titanium, or stainless steel to transport currents for electrochemical biofilm control.[16,19-21] These metals do not have high degrees of flexibility and the electrochemical systems created with them are not practical for topical wound applications. The use of copper wire in electrochemical systems is relatively understudied, despite its natural biocidal properties. Copper atoms can oxidize in the presence of moisture and generate hydroxyl radicals *in situ*, which damage structural proteins that are vital for cellular function.[22,23] Similar to the mechanisms behind ROS toxicity, copper ions can break down bacterial cell walls, impair cellular respiration, and denature DNA.[24,25] Copper reduces the rate of horizontal gene transfer, which is the primary mechanism behind the rapid spread of virulence factors and antibiotic resistance in bacteria.[26] There is a

Stockholm International Youth Science Seminar is a part of Unga Forskare.

gap in literature discussing the use of copper electrodes that actively participate in disruptive chemical reactions while conducting electricity to kill bacteria. This study aims to create a more effective treatment for antibiotic-resistant bacteria that relies on a combination of electrical and ion therapy applied through a flexible bandage-like material.

Bacterial Cellulose for Wound Healing

Bacterial cellulose (BC) is a biopolymer $(C_6H_{10}O_5)_n$ synthesized at the air-liquid interface by the bacteria *Komagataeibacter sucrofermentans*.[27] BC is composed of intertwined and overlapping cellulose ribbons that are continuously produced by surface pores. These settle into microfibers and are pushed down into culture media below.[28] The fibers possess both amorphous and crystalline regions; the former regions are responsible for the material's flexibility and the latter endow high tensile strength to cellulose constructs.[29,30] The polymer is chemically identical to plant-produced cellulose but has a higher chemical purity and its microfibers are around 1,000 times finer.[31] Hydrogen bonds can stabilize the cellulose chains, allowing hydroxyl groups to tightly bind to water molecules.[32] This quality enables BC to maintain moisture concentrations that are optimal in wound healing.[33,34] The microfiber structure of BC acts as a biomimetic extracellular matrix of epidermal tissue.[34,35] In addition, epithelial cell migration can be directed along charge gradients between electrodes in an event known as electrotaxis.[36,37] Electroactive BC could harness both of these properties to promote wound closure while eradicating infection. Other biopolymers for wound dressing (*e.g.,* gelatin and chitosan) share numerous properties with BC like water retention and biocompatibility with BC. However, BC establishes superiority over many conventional materials used for wound healing due to its unique combination of bioactive properties.[28,32,38-40] Most of the current literature focuses on applying BC to non-infected wounds to accelerate the healing process. This study seeks to use BC as the structural element of a bandage to eradicate antibiotic-resistant infection. BC is not electrically conductive because it holds its electrons tightly in a covalent network structure. For electrochemical therapy to be applied through a BC-based bandage, electrons must be able to flow efficiently.

Multiwalled Carbon Nanotubes

Integrating small conductive compounds like multi-walled carbon nanotubes (CNTs) could facilitate electrical conductivity in BC scaffolds. Unlike the carbon atoms in BC, CNTs are made of concentric graphite sheets that have an abundance of pathways for delocalized electrons.[41] This makes them one of the most electrically conductive materials at room temperature.[42] When subject to vigorous stretching and bending, CNT conductivity is not greatly compromised as it is for many conductive metals.[43] CNTs are also biocompatible for human tissue while toxic to bacterial cells.[44,45] This is significant because a bandage that is conductive and flexible is optimal for an electricidal wound dressing. This research seeks to determine if the application of an electrical current through BC processed with CNTs is an effective treatment against antibiotic-resistant *S. aureus*, and if the antimicrobial properties of oxidized copper and electrified BC work together in synergy to inhibit biofilm growth. Developing a BC-based wound dressing could compensate for the lack of treatments for chronic wounds and antibiotic resistance at once.

Methods

BC-CNT Synthesis

Komagataeibacter sucrofermentans ATTC Strain No. 700178 was used to produce a cellulose layer at the air-media interface. Precultures were prepared by transferring a small volume of *K. sucrofermentans* from a frozen stock to a Henstrin-Schramm liquid media (HS) in sterile Erlenmeyer flasks at room temperature and static conditions. After 3 days, sterile 24-well plates were filled with 2.5 mL of HS and 250 µL of preculture per well. After 7 days, BC pellicles were harvested and transferred into 200 mL Griffin beakers with 150 mL of distilled water. The samples were placed in a 60°C vacuum oven for 2 hours. The supernatant was then drained, and the samples were submerged in a 2% NaOH solution for 24 hours. The BC pellicles were then subjected to rinse and wash cycles to neutralize the pH and expel *K. sucrofermentans* carcasses. After sterilization, the polymer was designated as Pristine BC. Pristine BC pellicles were placed in conical tubes containing a CNT solution composed of Nink-1000 COOH functionalized MWCNTs and a surfactant in distilled water. The samples were then subjected to 48 hours of rotational incubation followed by lyophilization and designated as BC-CNT. BC-CNT composites were then rehydrated in a NaCl solution that contained different concentrations of vancomycin before use in electrochemical treatment.

Electrochemical Treatment of *S. aureus*

Staphylococcus aureus GFP strain RN4220+pCM 29 was inoculated in 10 mL of autoclaved ultrafine-yeast extract media (UFTYE, pH 7; Bacto Tryptone, Bacto Yeast Extract) in a sterile test tube for 24 hours at 37°C with orbital shaking. Cultures were centrifuged, the supernatant was discarded, and cell pellets were resuspended and diluted in a NaCl solution to reach optical density at 600 nm. Optical density (OD) readings around 0.6 a.u. recorded with a spectrophotometer and used in experiments. *S. aureus* suspension was pipetted onto a circular UFTYE agar disc surrounded by polydimethylsiloxane (PDMS). BC-CNT with copper (Cu) wire threaded through one side was placed over the *S. aureus*-coated agar. Titanium (Ti) wire was shaped into a semicircle and placed on the opposite side. Both wires were then connected to a potentiostat. The Cu working electrode (W.E.) collected current levels and was connected to the sense electrode (S.E.) that measured the voltage with respect to the reference electrode (R.E.). The Ti counter electrode (C.E.) controlled the power output of the potentiostat and was connected to the R.E. that controlled the voltage with respect to the S.E. The PDMS and all electrodes were sterilized before treatment. An electrolyte solution was pipetted on top of the BC-CNT prior to treatment. Voltage potentials were applied for 1 hour to produce varying current densities through the BC-CNT composites. A subset of experiments was conducted on UFTYE agar discs containing phenol red as a pH indicator. After electrochemical treatment was applied through BC-CNT on top, the phenol red agar

discs were imaged. To determine *S. aureus* susceptibility to vancomycin, a cell suspension was pipetted into UFTYE liquid culture media in a 96-well plate. The cells were exposed to a serial dilution of vancomycin and incubated at 37°C. Optical density (OD) absorbance readings were collected every hour over a 48-hour time interval, and the minimum inhibitory concentration was identified from graphical analysis.

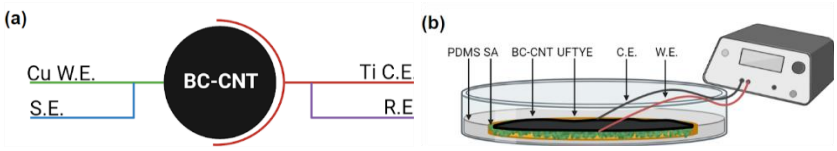

Figure 1. Schematic diagrams of the electrochemical cell setup. (a) top view of BC-CNT with all electrode components. (b) side view with two-terminal connections used for electrochemical treatment of *S. aureus*.

S. aureus Quantificaiton

After treatment for 1 hour, the BC-CNT electrochemical cell was deconstructed. BC-CNT and the corresponding UFTYE agar disc were incubated at 37°C in static conditions. For whole-sample macroscopic imaging, a light source was used to illuminate *S. aureus*, and a barrier filter allowed wavelengths to be detected by a camera. To quantify the fluorescent intensity of *S. aureus* on UFTYE discs and BC-CNT composites, Fiji software was used. Images were processed, and the area of the sample under the threshold mask was calculated to determine the size of the *S. aureus* biofilm. To further analyze the impacts of the electrochemical treatment on *S. aureus* at a cellular level, scanning electron microscopy (SEM) was conducted.

CNT Loading and Release from BC-CNT

A CNT-loading and release profile of BC-CNT was created using spectrophotometry. A stock solution of the Nink-1000 COOH functionalized MWCNTs were sonicated, and the solution was serially diluted to create concentrations ranging from µg/mL to µg/mL in a NaCl buffer. The solutions, in addition to a NaCl blank, were transferred into semi-micro cuvettes for absorbance readings at specified wavelengths, collected by a UV-Vis spectrophotometer. This data was analyzed to create a calibration curve for CNTs, mapping absorbance to a corresponding concentration. The amount of CNTs loaded into BC-CNT was determined by collecting absorbance values of CNT solutions before and after processing with BC. The loss of CNTs in the loading supernatant was present within BC-CNT composites. To create the release profile, dehydrated BC-CNT samples were placed into semi-micro cuvettes containing a NaCl buffer and were immediately loaded into the spectrophotometer. Absorbance readings were collected at specified intervals for 24 hours.

Results

CNT Integration and Stability in BC-CNT

UV-Vis spectrophotometry was used to quantify CNT loading and release from BC-CNT. A CNT absorbance peak was identified at 340 nm (Figure 3a) and used to generate a linear regression relating absorbance at 340 nm to CNT concentration in solution (Figure 3b). A linear regression represents the relationship between absorbance and CNT concentration, where y(A.U.) =0.0913x(µg/mL) + 0.0183. The coefficient of determination $R^2 = 1$ indicates direct proportionality between absorbance and concentration. Absorbance values at a 340 nm wavelength of the CNT suspension used to fabricate BC-CNT were collected before processing and processing loading, which involved submerging pristine BC in a 5% CNT solution followed by 2 hours of sonication and 48 hours of rotational incubation at 80 rpm. These absorbance values were converted to CNT concentration in solution with the equation generated in Figure 3b. After the CNT loading process, pristine BC lost its white coloration. BC-CNT takes on a dark black shade that illustrates substantial CNT uptake in the membrane (Figure 2c and 2d). The absolute value of the change in CNTs in solution after loading is assumed to be the amount of CNTs loaded into BC-CNT (Figure 2e). Absorbance readings at 340 nm were collected from cuvettes containing a 154 mM solution and one whole BC-CNT composite at the top of each cuvette, suspended well above the light path. Using the linear model generated in Figure 3b, absorbance values were charted to the corresponding CNT amount released over 24 hours (Figure 3f). The minimal CNT release from BC-CNT reveals that the CNTs are well adhered to the BC surface fibers. The higher rate of CNT release in the first 2 hours could be an initial shedding of loosely connected CNTs on the outer layer in BC-CNT. Once this subgroup of CNTs is dislocated, the amount of CNTs released slightly increases over time in a controlled manner. Overall, this release is relatively minimal but should be minimized to prevent CNTs from entering the body in later clinical trials. While excess CNT release could harm the delicate wound environment, the predictable release of BC-CNT makes the material suitable for further investigation into bandage applications. SEM imaging reveals BC is composed of intertwined and overlapping cellulose ribbons (Figure 2g).

Effects of Electrical Potential and Species on *S. aureus* Fitness

Whole sample imaging was used to quantify reductions in *S. aureus* fitness because of treatment with various voltage potentials and vancomycin concentrations in BC-CNT (Figure 3). UFTYE represents the wound and BC-CNT is the bandage in this model. The phenol red column in Figure 4b indicated a pH of 7 in the electrochemical system when a 0 V potential was applied. There is an area of inhibited growth in the leftmost portion of 0 V BC-CNT with 0 µg/mL and 3.125 µg/mL of vancomycin. Because no voltage potential was used in these tests, the site of killing around the copper working electrodes could mean that the 154 mM NaCl electrolyte oxidizes the Cu wire and releases

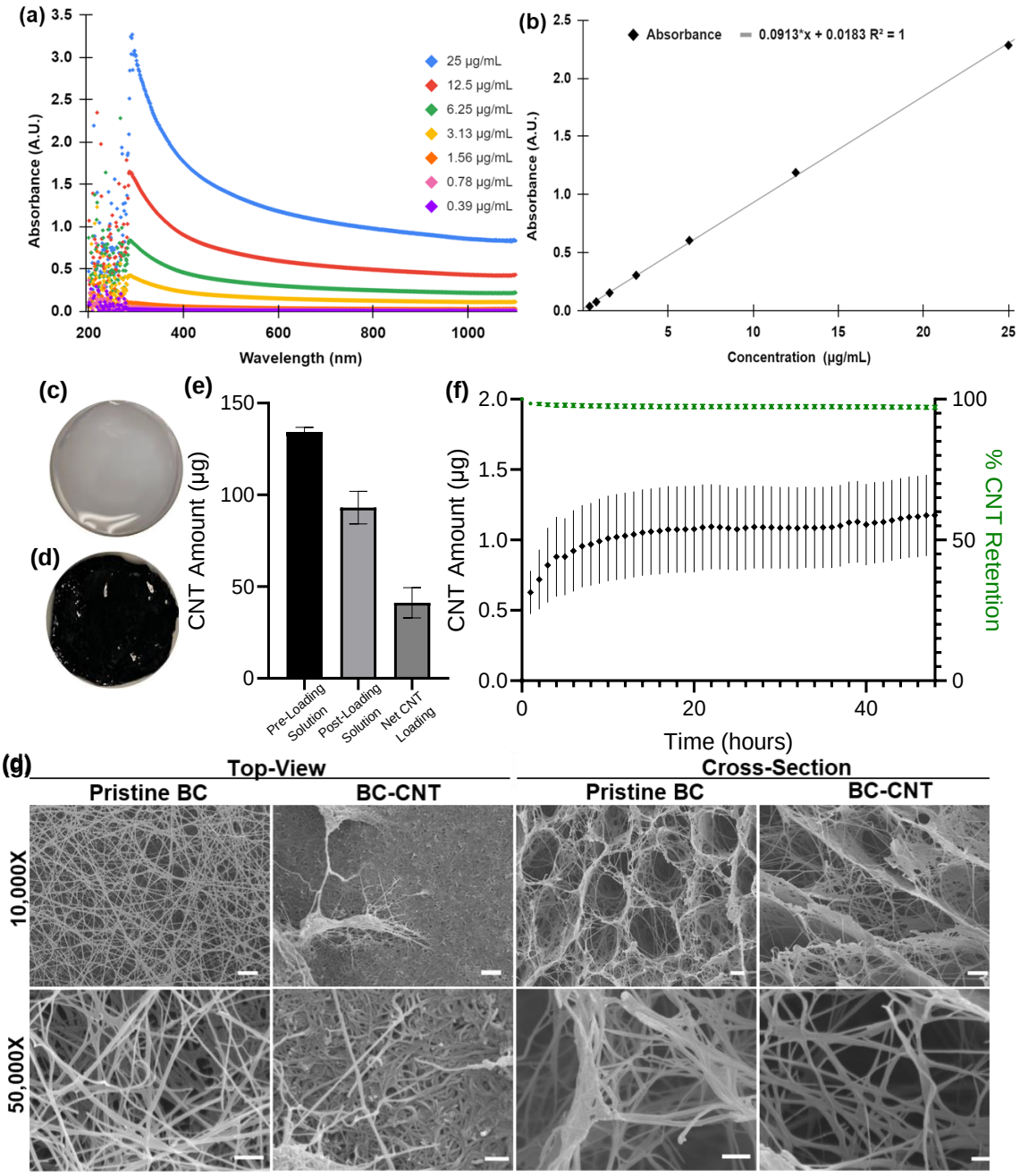

copper ions with bactericidal effects. When treated with 2.5 V, the violet hue around the Ti C.E. terminal connection indicates a slightly basic pH of 8. The yellowing of the phenol red around the Cu working electrode shows a reduction in pH to around 6. Electrochemical reactions are responsible for these changes because BC-CNT and the Cu terminal connection do not innately influence the pH of the system (Figure 3). Currents originating

Figure 2. (a) Absorbance values across 250-1100 nm wavelengths for serially diluted CNTs. (b) CNT calibration plot generating linear regression relating absorbance to CNT concentration in solution at 340 nm wavelength. (c) Pristine BC and (d) BC-CNT both hydrated with an aqueous 154 mM NaCl solution. (e) Average amount of CNT loaded into BC-CNT after 48 hours in 5% CNT solution ± standard deviation. (f) Average CNT release from BC-CNT over 24 hours. (g) SEM images of top-view and cross-sectional fibers in Pristine BC and BC-CNT at 10,000X (scale bar = 1 nm) and 50,000X (scale bar = 2 µm).

from the W.E. are strong enough to drive water hydrolysis. Oxygen can form hydroxyl radicals after accepting free electrons generated during redox reactions between the W.E. and C.E. These processes contribute to the formation of acidic ROS including H_2O_2 (pH ~6) during treatment. The dark areas of UFTYE and BC-CNT after treatment with 2.5 V and 5 V are locations in which *S. aureus* was either killed or severely damaged by the electrochemical treatment to the point where the bacteria could not recover after 24 hours. After exposure to 2.5 V and 5 V with 0 µg/mL of vancomycin, killing is relegated to the acidified area around the working electrode. The consistency of this area of inhibited growth across conditions indicates a high degree of cell damage at the W.E. due to ROS exposure, which induces oxidative stress, and mutates DNA, leading to cell lysis.[47] This evidence suggests ROS alone is a killing mechanism from the electrochemical bandage. This compromised *S. aureus* recovery due to ROS exposure is quantified in Figure 4c.

Bactericidal Synergy Between Electricity and Antibiotics

The higher degree of killing seen when the antibiotic was used in conjunction with electricity indicates that electroactive BC-CNT composites can greatly enhance *S. aureus* susceptibility to the concentration vancomycin it was initially resistant to. This evidence indicates that vancomycin and ROS work in synergy to eradicate *S. aureus*. ROS could disrupt the membrane permeability and potential of *S. aureus*, which could render the cell's membrane-dependent form of vancomycin evasion unsuccessful. After electrochemical treatment, *S. aureus* is unable to control the flow of small molecules through its membrane, which is seen in Figure 4d as an increase in the extrusion of cellular debris with voltage potential.

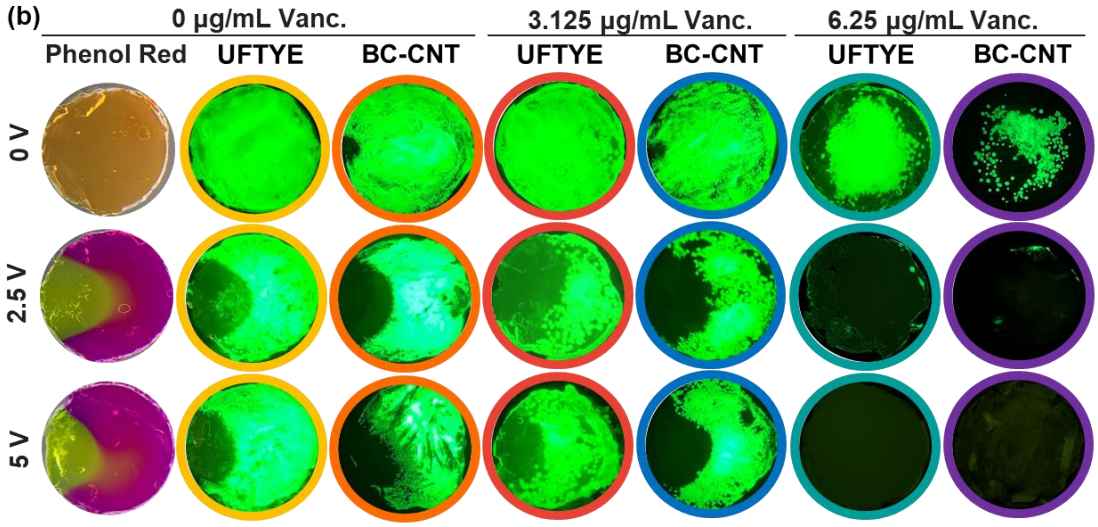

Figure 3. UFTYE and BC-CNT composites with fluorescing GFP *S. aureus* post-treatment.

Conclusions and Perspective

Analysis of BC-CNT Composites and Bactericidal Efficacy

The fabrication and testing of biosynthetic BC-CNT bandages in this research advance a new direction for overcoming antibiotic-resistant bacterial infections. SEM imaging shows a dense integration of CNTs onto the outer layers of BC, with porous inner structures remaining open for loading with electrolytes and antibiotics. Spectrophotometric analysis reveals limited CNT release from BC over time. Macroscopic fluorescent imaging of *S. aureus* after treatment demonstrates the capability of electrified BC-CNT to prevent biofilm formation of vancomycin-resistant *S. aureus*. Phenol red indicates electrochemically driven water hydrolysis forms ROS as a killing mechanism. The release of copper ions at the working electrode may be accelerated as treatment time lengthens because lower pH solutions increase the rate of Cu oxidation.[48] Combinatorial treatment of S. aureus with electroactive BC-CNT bandages loaded with vancomycin results in a biocidal synergy that re-sensitizes *S. aureus* to vancomycin, yielding an 83% and 91% reduction in total biofilm area on the UFTYE wound model and BC-CNT bandage.

Limitations and Future Directions

The in vitro studies of this project limit quantifications of wound healing capabilities and understandings of physiological interactions in the wound bed with BC-CNT bandages. Additional testing to confirm that electrochemical treatment through BC is only lethal to bacterial cells and safe for mammalian cells is needed before research with *in vivo* testing using animal models can take place. On average, electroactive BC-CNT had a current density of 450 µA/cm^2 which is below the threshold of human perceptibility. Nevertheless, using the lowest voltage potential possible that is still able to suppress *S. aureus* recovery is the safest option for patient health. Minimizing the potential used for treatment will reduce the possibility of electrical burns and interference with other medical devices.

Small variations in CNT distribution and amount across the BC-CNT composites used for testing could have either enhanced or reduced the bandage's electrical conductivity. Differences in conductivity could be responsible for the variability seen in *S. aureus* recovery between treatments. Additional processing such as pyrolysis will be carried out to improve the conductivity of BC-CNT before *in vivo* testing. Pyrolyzing BC through high temperatures, pressures, and flowing argon gas has been found to significantly enhance the conductivity of BC nanofibers by reorganizing their atomic structures.[48] This chemical modification exploits cellulose's hydroxyl groups, exposing aldehydes and carboxylic acids which allow for an increase of conductivity to take place.[49] When a BC-CNT is used in a wound bed, it is important that the amount of CNT released is as minimal as possible due to concerns over potential cytotoxicity. While BC-CNT was shown to be relatively stable, improvements to CNT incorporation can be made. Further optimization of the BC-CNT bandage could include barriers to prevent CNTs from exiting the apparatus. Multiple experiments are underway to characterize the material properties of the BC-CNT bandages. Electrochemical impedance spectroscopy will allow for quantifiable reductions in BC resistivity to be made. Fourier transform infrared spectroscopy is being conducted to determine the bonding interaction between BC and CNTs and x-ray diffraction and transmission electron microscopy is

providing insight into microstructural changes caused by CNT integration. Understanding how this interaction can be enhanced to improve CNT adherence will contribute to the development of a more durable BC-CNT bandage. Transmission electron microscopy is in progress to better understand how individual CNTs interact with BC microfibers. Further research is needed to elucidate the molecular mechanisms behind the electrochemical control of *S. aureus*. Live-dead stains, transcriptomics, and optogenetic analysis could be used to better understand how the treatment impacts cellular functions. In addition, cyclic voltammetry and liquid chromatography could be used to identify the reactive oxygen species produced during treatment.

Research Value and Outlook

Bacteria are constantly evolving new mechanisms to evade treatments developed by humans, so a multifaceted approach to combating antibiotic resistance requires a variety of therapies engaging in different techniques for eradication. Biofilms are also increasingly present on implantable medical devices made of metal, such as catheters. An exploration into applications of electrochemical therapy applied through these devices could expand treatments for persistent infection in areas other than topical wounds. With these limitations addressed in future experiments, this project lays the groundwork for a new BC-based treatment for antibiotic-resistant biofilm infection through CNT-mediated electrical therapy that has not been previously established.

References

[1] O'Neill, J. Tackling Drug-Resistant Infection Globally: Final Report and Recommendations. *Review on Antimicrobial Resistance.* 2016. https://amr-review.org/sites/default/files/160518_Final%20paper_with%20cover.pdf

[2] Murray, C. L. J. *et al*. Global Burden of Bacterial Antimicrobial Resistance in 2019: a Systematic Analysis. *Lancet*. 399, 629-655. DOI: 10.1016/S0140-6736(21)02724-0

[3] Bessa L. J., Fazii, P., Giulio, M. D., & Cellini, L. Bacterial Isolates from Infected Wounds and their Antibiotic Susceptibility Pattern: Some Remarks about Wound Infection. *Int Wound J.* 2015, 12(1), 47-52. DOI: 10.1111/iwj.12049

[4] Attinger, C., & Wolcott, R. Clinically Addressing Biofilm in Chronic Wounds. *Adv. Wound Care*. 2012, 1(3), 127-132. DOI: 10.1089/wound.2011.0333

[5] Luppens, S. B. I., Reij, M. W., van der Heijden, R. W. L., Rombouts, F. M., & Abee, T. Development of a Standard Test to Assess the Resistance of *Staphylococcus aureus* biofilm cells to disinfectants. *Appl. Environ. Microbiol.* 2002, 68(9), 4194-4200. DOI: 10.1128/AEM.68.9.4194-4200.2002

[6] Mah, T. Biofilm-Specific Antibiotic Resistance. *Future Medicine.* 2012, 7(9). DOI: https://doi.org/10.2217/fmb.12.76

[7] Whitchurch, C. B., Tolker-Nielsen, T., Ragas, P. C., Mattick, J. S. Extracellular DNA Required for Bacterial Biofilm Formation. *Science.* 2002, 295(5559), 1487. DOI: 10.1126/science.295.5559.1487

[8] Wang, L., Yuan, L., Li, Z-H., Zhang, X., Leung, K. M. Y.,Sheng, G-P. Extracellular Polymeric Substances (EPS) Associated Extracellular Antibiotic Resistance Genes in Activated Sludge Along the AAO process: Distribution and Microbial Secretors. *Sci. Total Environ.* 2022, 816, 151575. DOI: 10.1016/j.scitotenv.2021.151575

[9] Waters, E. M., Rowe, S. E., O'Gara, J. P., Conlon, B. P. Convergence of Staphylococcus *aureus* Persister and Biofilm Research: Can Biofilms Be Defined as Communities of Adherent Persister Cells? *PLoS Pathology*. 2016, 12(12), 1006012. DOI: 10.1371/journal.ppat.1006012

[10] Fisher, R. A., Gollan, B., Helaine, S. Persistent Bacterial Infections and Persister Cells. *Nat. Rev. Microbiol.* 2017, 15, 453–464. DOI: 10.1038/nrmicro.2017.42

[11] World Health Organization. 2019 Antibacterial Agents in Clinical Development: An Analysis of the Antibacterial Clinical Development Pipeline. 2019. https://apps.who.int/iris/bitstream/handle/10665/330420/9789240000193-eng.pdf

[12] Niepa, T. H. R., Gilbert, J. L., Ren, D. Controlling *Pseudomonas aeruginosa* Persister Cells by Weak Electrochemical Currents and Synergistic Effects with Tobramycin. *Biomaterials.* 2012, 33(30), 7356-7365. DOI: 10.1016/j.biomaterials.2012.06.092

[13] Sultana, S. T., Atci, E., Babuata, J. T., Falghoush, A. M. Snekvik, K. R. Call, D. R., & Beyenal, H. Electrochemical Scaffold Generates Localized, Low Concentration of Hydrogen Peroxide that Inhibits Bacterial Pathogens and Biofilms. *Sci. Rep.* 2015, 5, 14908. DOI: 10.1038/srep14908

[14] Wang, C., Yue, L., Wang, S., Pu, Y., Zhang, X., Hao, X., Wang, W., & Chen, S. Role of Electric Field and Reactive Oxygen Species in Enhancing Antibacterial Activity: A Case Study of 3D Cu Foam Electrode with Branched CuO–ZnO NWs. *J. Phys. Chem. C.* 2018, 122(46), 26454–26463

[15] Reipa, V., Atha, D. H., Coskun, S. H., Sims, C. H., Nelson, B. C. Controlled Potential Electro-Oxidation of Genomic DNA. *PLoS ONE*. 2018, 13(1), 0190907. DOI: 10.1371/journal.pone.0190907

[16] Zhang, J., Neoh, K. G., Hu, X., Kang, E-T. Mechanistic Insights Into Response of *Staphylococcus aureus* to Bioelectric Effect on Polypyrrole/Chitosan Film. *Biomaterials*. 2014, 35(27), 7690-7698. DOI: 10.1016/j.biomaterials.2014.05.069

[17] Krishnamurthi, V. R., Rogers, A., Peifer, J. Niyonshuti, I. I., Chen, J., & Wang, Y. Microampere Electrical Current Causes Bacterial Membrane Damage and Two-Way Leakage in a Short Period of Time. *Appl. Environ. Microbiol.* 2020, 86(16), 01015-010120. DOI: 10.1128/AEM/01015-20

[18] Parry-Nweye, E., Onukwugha, N-E., Balmuri, S. B., Shane, J. L., Kim, D., Koo, H., & Niepa, T. H. R. Electrochemical Strategy for Eradicating Fluconazole-Tolerant *Candida albicans* Using Implantable Titanium. *ACS Appl. Mater. Interfaces.* 2019, 11(44), 40997-41008. DOI: 10.1021/acsami.9b09977

[19] Sultana, S. T., Call, D. R., Beyenal, H. Eradication of *Pseudomonas aeruginosa* Biofilms and Persister Cells Using an Electrochemical Scaffold and Enhanced Antibiotic Susceptibility. *npj Biofilms Microbiomes*. 2016, 2(2). DOI: 10.1038/s41522-016-0003-0

[20] de Pozo, J. L., Rouse, M. S., Mandrekar, J. N., Sampedro, M. F., Steckelberg, J. M., & Patel, R. Effect of Electrical Current on the Activities of Antimicrobial Agents against *Pseudomonas aeruginosa*, *Staphylococcus aureus*, and *Staphylococcus epidermidis* Biofilms. *Antimicrob. Agents Chemother.* 2009, 53(1), 35-40. DOI: 10.1128/AAC.00237-08

[21] Nowruzi, F., Imani, R. & Faghihi, S. Effect of Electrochemical Oxidation and Drug Loading on the Antibacterial Properties and Cell Biocompatibility of Titanium Substrates. *Sci. Rep.* 2022, 12, 8595. DOI: 10.1038/s41598-022-12332-z

[22] Warnes, S. L., Caves, V., Keevil, W. Mechanism of Copper Surface Toxicity in *Escherichia coli* O157:H7 and *Salmonella* Involves Immediate Membrane Depolarization Followed by Slower rate of DNA Destruction which Differs from that Observed for Gram-Positive Bacteria. *Enviro. Microbiol.* 2011, 14, 1730-1743. DOI: 10.1111/j.1462-2920.2011.02677.x

[23] Macomber, L., Imlay, J. A. The Iron-Sulfur Clusters of Dehydratases are Primary Intracellular Targets of Copper Toxicity. *Proc. Natl. Acad. Sci. USA.* 2009, 106(20), 8344-8349. DOI: 10.1073/pnas.0812808106

[24] Weaver, L., Noyce, J. O., Michels, H. T., Keevil, C. W. Potential action of copper surfaces on methicillin-resistant *Staphylococcus aureus*. *J. App. Microbiol.* 2010, 109(6), 2200-2205. DOI: 10.1111/j.1365-2672.2010.04852.x

[25] Warnes, S. L., Keevil, C. W. Lack of Involvement of Fenton Chemistry in Death of Methicillin-Resistant and Methicillin-Sensitive Strains of *Staphylococcus aureus* and Destruction of Their Genomes on Wet or Dry Copper Alloy Surfaces. *App. Enviro. Microbiol.* 2016, 82(7), 2132-2136. DOI: 10.1128/AEM.03861-15

[26] Buberg, M. L., Witsø, I. L., L'Abée-Lund, T. M., and Wasteson, Y. Zinc and Copper Reduce Conjugative Transfer of Resistance Plasmids from Extended-Spectrum Beta-Lactamase-Producing *Escherichia coli*. *Microb. Drug Resist.* 2020, 26(7), 842-849. DOI: 10.1089/mdr.2019.0388

[27] Brugnoli, M., Robotti, F., La China, S. *et al.* Assessing effectiveness of *Komagataeibacter* Strains for Producing Surface-Microstructured Cellulose via Guided Assembly-Based Biolithography. *Sci. Rep.* 2021, 11, 1931. DOI: 10.1038/s41598-021-98705-2

[28] Bielecki, S., Krystynowicz, A., Turkiewicz, M., & Kalinowska, H. Bacterial Cellulose. *Biopolymers Online.* 2002, 5, 31-84. DOI: 10.1002/3527600035.bpol5003

[29] Kolakovic, R., Peltonen, L., Laukkanen, A., Hirvonen, J., & Laaksonen, T. Nanofibrillar Cellulose Films for Controlled Drug Delivery. *Eur. J. Pharm. Biopharm.* 2012 ,82(2), 308-315. DOI: 10.1016/j.ejpb.2012.06.011

[30] Guhados, G., Wan, W., & Hunter, J. L. Measurement of the Elastic Modulus of Single Bacterial Cellulose Fibers Using Atomic Force Microscopy. *Langmuir.* 2005, 21(14), 6642-6646. DOI: 10.1021/la0504311

[31] Freire, C. S. R., Fernandes, S. C. M., Silvestre, A. J. D., & Neto, C. P. Novel Cellulose-Based Composites Based on Nanofibrillated Plant and Bacterial Cellulose: Recent Advances at the University of Aveiro - a Review. *Holzforschung.* 2013, 67(6), 603-612. DOI: 10.1515/hf-2012-0127

[32] Portela, R., Leal, C. R., Almeida, P. L., & Sobral, R. G. Bacterial Cellulose: A Versatile Biopolymer for Wound Dressing Applications. *Microb. Biotechnol.* 2019, 12(4), 1-25. DOI: 10.1111/1751-7915.13392

[33] Schrecker, S. T., & Gostomski, P. A. Determining the Water Holding Capacity of Microbial Cellulose. *Biotechnol. Lett.* 2005, 27, 1435-1438. DOI: 10.1007/s10529-005-1465-y

[34] Cherng, J. H., Chou, S. C., Chen, C. L., Wang, Y. W., Chang, S. J., Fan, G. Y., Leung, F. S., & Meng, E. Bacterial Cellulose as a Potential Bio-Scaffold for Effective Re-Epithelialization Therapy. *Pharmaceuticals.* 2021, 13(10), 1592. DOI: 10.3390/pharmaceutics13101592

[35] Li, Y., Wang, S., Huang, R., Huang, Z., Hu, B., Zheng, W., Yang, G., Jiang, X. Evaluation of the Effect of the Structure of Bacterial Cellulose on Full Thickness Skin Wound Repair on a Microfluidic Chip. *Biomacromolecules.* 2015, 16, 780–789. DOI: 10.1021/bm501680s

[36] Korupalli, C., Li, H., Nguyen, N., Mi, F-L., Chang, Y., Lin, Y-J., & Sung, H-W. Conductive Materials for Healing Wounds: Their Incorporation in Electroactive Wound Dressings, Characterization, and Perspectives. *Adv. Healthcare Mater.* 2021, 10(6), 2001384. DOI: 10.1002/adhm.202001384

[37] Guo, A., Song, B., Reid, B., Gu, Y., Forrester, J. V., Jahoda, C. A.B., & Zhao, M. Effects of Physiological Electric Fields on Migration of Human Dermal Fibroblasts. *J. Invest. Dermatol.* 2010, 130(9), 2320-2327. DOI: 10.1038/jid.2010.96

[38] Zheng, Lu., Li, S., Luo, J., & Wang, X. Latest Advances on Bacterial Cellulose-Based Antibacterial Materials as Wound Dressings. *Front. Bioeng. Biotechnol.* 2020, 8, 593768. DOI: 10.3389/fbioe.2020.593768

[39] Ahmed, J., Gultekinoglu, M., & Edirisinghe, M. Bacterial Cellulose Micro-nano Fibers for Wound Helping Applications. *Biotechnol. Adv.* 2020, 41, 107549. DOI: 10.1016/j.biotechadv.2020.107549

[40] Sulaeva, I., Henniges, U., Rosenau, T., & Potthast, A. Bacterial Cellulose as a Material for Wound Treatment: Properties and Modifications. *Biotechnol. Adv.,* 2015, 33(8), 1541-1571. DOI: 10.1016/j.biotechadv.2015.07.009

[41] Forro, L., & Schonenberger, C. Physics of Multiwalled Carbon Nanotubes. *Physics, Chemistry, and Applications of Nanostructures.* 2001. DOI: https://doi.org/10.1142/9789812810076_0010

[42] Poncharal, P., Berger, C., Yi, Y., Wang, Z. L, & de Heer, W. A. Room Temperature Ballistic Conduction in Carbon Nanotubes. *J. Phys. Chem. B.* 2002, 106(47), 12104-12118. DOI: 10.1021/jp021271u

[43] Bulmer, J, S., Kaniyoor, A., Elliott, J, A. A Meta-Analysis of Conductive and Strong Carbon Nanotube Materials. *Adv. Mater. 2021,* 33(36), 2008432. 10.1002/adma.202008432

[44] Khan, F.S.A., Mubarak, N.M., Khalid, M. *et al*. Functionalized Multi-walled Carbon Nanotubes and Hydroxyapatite Nanorods Reinforced with Polypropylene for Biomedical Application. *Sci. Rep.* 2021, 11, 843. DOI: 10.1038/s41598-020-80767-3

[45] Bai, Y., Park, I. S., Lee, S. J., Bae, T. S., Uo, F. W. M., Lee, M. H. Aqueous dispersions of surfactant-modified multiwalled carbon nanotubes and their application as an antibacterial agent. *Carbon*. 2011, 49, 11. DOI: 10.1016/j.carbon.2011.05.002

[46] Princeton Applied Research. VersaSTAT 3 Hardware Manual. *AMETEK*. 2021 https://www.ameteksi.com/-/media/ameteksi/download_links/documentations/supportcenter/princetonappliedresearch/howtoguides/versastudio_quick_start_guide.pdf?revision=74c9c8f7-063f-411f-bf16-3f7b2c3c8a78

[47] Davis, J. M., & Auten, R, L. Oxygen Toxicity and Reactive Oxygen Species: the Devil is in the Details. *Pediatric Res.* 2009, 66, 121-127. DOI: 10.1203/PDR.0b013e3181a9eafb

[48] Mora, N., Cano, E., Mora, E. M., & Bastidas, J. M. Influence of pH and oxygen on copper corrosion in simulated uterine fluid. Biomaterials, 2001, 23(3), 667-671. DOI: 10.1016/S0142-9612(01)00154-5.

[49] Liang, A-W., Guan, Q-F., Zhu, Z., Song, L-T., Yao, H-B., Lei, X., & Yu, S-H. (2012). Highly Conductive and Stretchable Conductors Fabricated from Bacterial Cellulose. *NPG Asia Mater.* 2012*,* 4, e19. https://doi.org/10.1038/am.2012.34